

Electron-Impact Ionization and Dissociative Ionization of the CD_3 and CD_2 Free Radicals

Frank A. Baiocchi, Robert C. Wetzel, and Robert S. Freund

AT&T Bell Laboratories, Murray Hill, New Jersey 07974

(Received 27 April 1984)

Absolute cross sections and mass-spectral cracking patterns are reported for ionization of the free radicals CD_3 and CD_2 . Such data for free radicals have previously been unmeasured because of their high reactivity. In this work, a beam of pure free radicals is generated by charge-transfer neutralization of a fast ion beam and is ionized by a crossed electron beam. With this approach, complete collection of mass-selected parent and fragment ions is obtained, permitting measurement of quantitative cross sections.

PACS numbers: 34.80.Gs, 07.75.+h, 82.20.Ms

Despite the numerous measurements made of ionization potentials and mass-spectral cracking patterns, quantitative ionization cross-section measurements remain scarce.^{1,2} The available cross-section data are mainly for ionization of atoms, atomic ions, and small molecules. For *dissociative* ionization (the formation of fragment ions) of molecules, there have been very few reliable cross-section measurements. This is primarily because dissociation imparts several electronvolts of translational energy to the fragments, making it difficult to collect 100% of each fragment. The lack of data is even more extreme when the molecule is a free radical; only a few relative measurements exist.³ Yet such cross sections are needed to better understand and model the discharges used for etching⁴ and depositing³ semiconductor materials and to analyze mass spectra of free radicals.⁵

We report the first of a series of free-radical ionization cross-section measurements. The free radicals studied are deuterated methyl (CD_3) and methylene (CD_2)—the deuterated species being chosen to provide better mass resolution relative to protonated species. We use a crossed-beams apparatus⁶ (Fig. 1) with two novel features: (1) a pure fast beam of free radicals (that is, no other chemical species are present) generated by charge-transfer neutralization of a mass-selected ion beam, and (2) mass selection and complete collection of fragment ions, made possible by the strong forward scattering of the fragments in the laboratory frame.

The free-radical source follows Peterson's design.⁷ Ions are extracted from a dc discharge source (Colutron model 100), accelerated to 500–3000-eV energy, mass selected by a Wien velocity filter, and then passed through a low-pressure gas cell. Resonant charge-transfer neutralization gives a beam of neutral free radicals with the same velocity as the ion beam. Radical trajectories are unchanged from those of the ions because resonant

charge-transfer collisions occur predominantly at large impact parameters with negligible momentum transfer. Neutral products scattered at larger angles are removed by collimating apertures. Ions passing through the gas cell are deflected out of the beam and monitored.

Source conditions were empirically optimized for maximum beam intensity. 1-keV CD_3^+ and CD_2^+ beams were extracted from a 1:1 $CD_4:D_2$ discharge, a mixture which gave good source stability. Cyclopropane (ionization potential $V_I=10.1$ eV) and allene ($V_I=9.5$ eV) were used to neutralize CD_2^+ and CD_3^+ , respectively, with approximate charge-transfer cross sections of 15 and 25 \AA^2 for formation of CD_2 ($V_I=10.4$ eV) and CD_3 ($V_I=9.6$ eV). Less intense beams were also generated with ethylene ($V_I=10.5$ eV), ethane ($V_I=11.5$ eV),

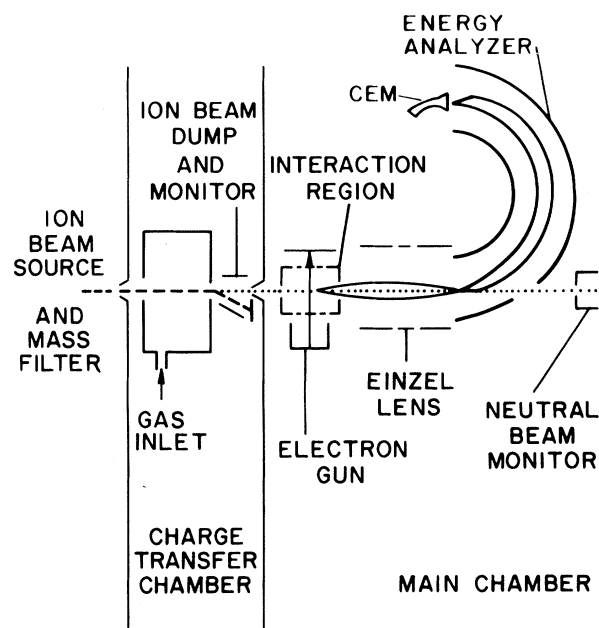


FIG. 1. Apparatus schematic.

and CD_4 ($V_f = 13.0$ eV) as charge-transfer gases. Efficient ion beam neutralization was not critically dependent on matching the ionization potentials of the charge-transfer partners.

The ionization cross section as a function of electron energy, $\sigma(E)$ (in square centimeters), is given for a crossed-beam configuration by²

$$I_i(E) = \sigma(E) I_e F(E) R \\ \times [(v_e^2 + v_n^2)^{1/2} / v_n v_e],$$

where $I_i(E)$ and $I_e(E)$ are the ion and electron currents, respectively, v_e and v_n are the electron and neutral beam velocities, respectively, R is the neutral beam flux (in particles/second), and $F(E)$ is a measure of the overlap of the two beams (in reciprocal centimeters).

The current of parent or fragment ions, $I_i(E)$, is measured by mass selecting the desired ions on the basis of their kinetic energy by a hemispherical electrostatic energy analyzer (mass resolution of 20), and collecting them quantitatively on a channel electron multiplier (CEM). Fragment ions may acquire several electronvolts of kinetic energy from the dissociation process; this defocuses the beam and introduces an energy spread. An einzel lens placed between the interaction region and the hemispherical energy analyzer refocuses the beam. The energy spread in this case limits the mass resolution to a value of ~ 12 . Complete collection of all carbon-containing ions was demonstrated by sweeping the beam horizontally across the CEM face; the ion beam width inferred from these data shows that the beam is smaller than the CEM diameter. Finally, the detector efficiency must be known to convert its output to an ion current. We operate the CEM in the pulse-counting mode. Varying the energies of the ions striking the CEM and varying the CEM gain produce no change in count rate. This indicates near unit efficiency and is consistent with previous measurements of similar CEM's.⁸

The electron current, $I_e(E)$, is typically 100–200 μA . The electron gun follows a pentode vacuum tube design, with the screen grid replaced by two grids defining the interaction-region potential. After intersecting the neutral beam, electrons are collected on the top interaction-region grid, the suppressor grid, and the anode plate. The upper two electron-gun elements are biased to prevent secondary and reflected electrons formed at these surfaces with less than 60-eV energy from entering the interaction region. Low-energy secondary electrons possibly formed at the electron-beam-defining

aperture (the bottom interaction region grid) were not observed in a retarding-potential analysis.

The neutral-beam flux, R , is measured by monitoring the secondary electrons emitted when the fast neutral beam hits a metal (Nichrome) surface. The secondary yield of the surface is calibrated before each measurement by use of a pyroelectric detector.⁹ The secondary-electron monitor and pyroelectric detector are over 3 cm in diameter, large enough to collect the entire beam. A neutral flux of $\sim 10^{10} \text{ s}^{-1}$ is common.

The overlap factor, F (as defined by Ref. 2), is calculated from measured profiles of the electron and neutral beams. The neutral beam is narrower than the electron beam with their relative positions determined by rectangular apertures. A stopwire scanned across the neutral beam has demonstrated its uniformity. The electron-beam distribution is continuously sampled with use of ten equally spaced narrow slots in the anode.

Background is due almost entirely to ionization of the fast neutrals by collision with the 5×10^{-8} -Torr background gas. Signal is distinguished from background by modulating the electron beam and the neutral beam. Drifts in experimental parameters do not affect the cross-section measurements because electron energy scans are done under computer control with $I_i(E)$, $I_e(E)$, F , and R measured for each value of E .

A series of apparatus checks were done by comparing cross sections measured for He, Ne, Ar, and Kr to published values. The ionization efficiency curve for Ne, the rare gas closest in mass to CD_3 and CD_2 , agrees in shape to better than 5% with literature data¹⁰ from threshold to 200 eV. Measurements of the absolute ionization cross section for Ne fell reproducibly within $\pm 30\%$ of the accepted value. This agreement is typical of that found for the other rare gases.

The results for the ionization cross sections of CD_3 and CD_2 are presented in Fig. 2. Ionization to the parent ion is the dominant process in each case, with the next most probable process being dissociative ionization with the loss of one deuterium atom. The lighter carbon-containing fragment ions were observed to have maximum cross sections less than 15% of the parent-ion cross sections, but they were not measured carefully at this time because the signal level was small with respect to the statistical fluctuations of the background.

The cross-section ratio of fragment production to parent-ion production is fairly constant over an electron energy range of 50–200 eV, with a value of 0.65 ± 0.06 for CD_3 and 0.39 ± 0.04 for CD_2 at an

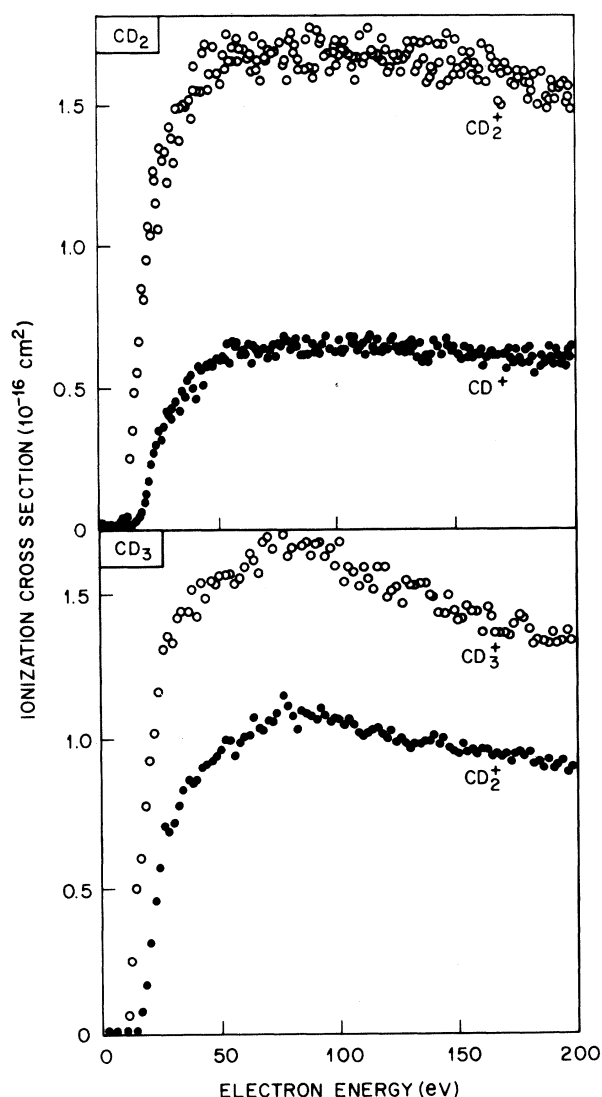


FIG. 2. Ionization cross sections for formation of CD_2^+ and CD_3^+ from CD_3 , and CD^+ and CD_2^+ from CD_2 .

energy of 100 eV. This ratio is the equivalent of a mass-spectrometric cracking pattern. It can be measured more accurately than either absolute cross section since it does not require absolute measurements of $I_e(E)$, $F(E)$, and R . The errors in these ratios are based on statistical uncertainties in the relative cross sections of 3% for CD_3 and 5% for CD_2 , and an estimated 10% uncertainty due to the possibly different CEM efficiencies for the parent and fragment ions.

The absolute ionization cross sections for CD_3 and CD_2 are given in Fig. 2. Statistical uncertainties in each of the measured quantities required to calculate the cross section were combined in quadrature to give a $\pm 20\%$ error. The largest systematic

uncertainty is the Channeltron efficiency, which is estimated to be 20% on the basis of reported variations of efficiency with mass of the impinging particle.⁸ Hence, a combined error limit of $\pm 30\%$ is obtained for the absolute cross sections, a limit which is supported by the rare-gas calibrations.

Appearance-potential measurements confirm the identities of the radicals and put upper bounds on their internal energies. The agreement with literature values is well within experimental uncertainty. (No previous threshold measurement is available for the formation of CD^+ from CD_2 , but our result is consistent with a thermochemical calculation.) This agreement provides experimental evidence that the vibrational or metastable electronic levels populated in the CD_3 and CD_2 beams are within 0.5 eV of the ground state, the accuracy of the appearance potential measurements. Since the metastable 1A_1 state of CD_2 is only 0.4 eV above the 3B_1 ground state, the appearance-potential measurements cannot rule out the possibility that some metastable CD_2 is present in the beam.

Since cross sections for ionization of CH_4 have been published,¹¹ measurements on CD_4 were made to check the apparatus. However, the measured CD_4 appearance potentials are about 2 eV lower than literature values indicating ~ 2 eV of vibrational excitation. This internal excitation apparently affects the cracking pattern: We measure intensities of 100:400:200 for $CD_4^+ : CD_3^+ : CD_2^+$ formation from CD_4 at 100 eV, whereas the literature gives 100:85:15. This observed internal energy is explained by geometry differences between CD_4 and CD_4^+ at their potential minima.¹² The Franck-Condon factors favor neutralization from the ion ground state to neutral excited vibrational states. In contrast, CD_3^+ and CD_2^+ undergo minimal structural changes on neutralization to their *ground* electronic states,¹² so that their neutral species form in low vibrational levels.

In conclusion, we have measured the first absolute ionization and dissociative ionization cross sections of free radicals. CD_3 and CD_2 ionize primarily to their parent ions, but with significant cross sections for fragment ion formation. The method is accurate and reliable, as indicated by a number of tests and by remeasurement of the well-known rare-gas-atom ionization cross sections. This fast-beam method should be applicable to measurements of electron-impact ionization of many other radicals as well as of stable molecules. It could also be applicable to other collision processes such as electron-impact excitation and dissociation, and the corresponding single-photon and multiphoton

processes.

-
- ¹T. D. Märk, *Int. J. Mass Spectrom. Ion Phys.* **45**, 125 (1982).
- ²L. J. Kieffer and G. H. Dunn, *Rev. Mod. Phys.* **38**, 1 (1966).
- ³R. Robertson, D. Hils, H. Chatham, and A. Gallagher, *Appl. Phys. Lett.* **43**, 544 (1983).
- ⁴H. F. Winters, J. W. Coburn, and T. J. Chuang, *J. Vac. Sci. Technol. B* **1**, 469 (1983).
- ⁵H. F. Winters and F. A. Houle, *J. Appl. Phys.* **54**, 1218 (1983).
- ⁶E. Brook, M. F. A. Harrison, and A. C. H. Smith, *J. Phys. B* **11**, 3115 (1978).
- ⁷J. R. Peterson, in *Atomic Collision Processes*, edited by M. R. C. McDowell (North-Holland, Amsterdam, 1964), p. 465.
- ⁸W. E. Potter and K. Mauersberger, *Rev. Sci. Instrum.* **43**, 1327 (1972).
- ⁹R. H. McFarland, A. S. Schlachter, J. W. Stearns, B. Lin, and R. E. Olson, *Phys. Rev. A* **26**, 775 (1982).
- ¹⁰K. Stephan, H. Helm, and T. D. Märk, *J. Chem. Phys.* **73**, 3763 (1980).
- ¹¹B. Adamczyk, A. J. H. Boerboom, B. L. Schram, and J. Kistemaker, *J. Chem. Phys.* **44**, 4640 (1966).
- ¹²P. C. Hariharan and J. A. Pople, *Mol. Phys.* **27**, 209 (1974).